



Strategic basin and delta planning increases the resilience of the Mekong Delta under future uncertainty

R. J. P. Schmitt^{a,b,1}, M. Giuliani^c, S. Bizzi^{c,d}, G. M. Kondolf^e, G. C. Daily^{a,b,1}, and Andrea Castelletti^{c,f}

^aNatural Capital Project, Stanford University, Stanford, CA 94305; ^bThe Woods Institute for the Environment, Stanford University, Stanford, CA 94305; ^cDepartment of Electronics, Information, and Bioengineering, Politecnico di Milano, 20133 Milano, Italy; ^dDepartment of Geosciences, University of Padova, 35122 Padova, Italy; ^eDepartment of Landscape Architecture and Environmental Planning, University of California, Berkeley, CA 94720; and ^fInstitute of Environmental Engineering, ETH Zurich, 8049 Zurich, Switzerland

Contributed by G. C. Daily, July 26, 2021 (sent for review December 18, 2020; reviewed by Frances E. Dunn and Daniel Peter Loucks)

The climate resilience of river deltas is threatened by rising sea levels, accelerated land subsidence, and reduced sediment supply from contributing river basins. Yet, these uncertain and rapidly changing threats are rarely considered in conjunction. Here we provide an integrated assessment, on basin and delta scales, to identify key planning levers for increasing the climate resilience of the Mekong Delta. We find, first, that 23 to 90% of this unusually productive delta might fall below sea level by 2100, with the large uncertainty driven mainly by future management of groundwater pumping and associated land subsidence. Second, maintaining sediment supply from the basin is crucial under all scenarios for maintaining delta land and enhancing the climate resilience of the system. We then use a bottom-up approach to identify basin development scenarios that are compatible with maintaining sediment supply at current levels. This analysis highlights, third, that strategic placement of hydropower dams will be more important for maintaining sediment supply than either projected increases in sediment yields or improved sediment management at individual dams. Our results demonstrate 1) the need for integrated planning across basin and delta scales, 2) the role of river sediment management as a nature-based solution to increase delta resilience, and 3) global benefits from strategic basin management to maintain resilient deltas, especially under uncertain and changing conditions.

Mekong | river deltas | resilience | sediment | global environmental change

By 2050, 1 billion people will live in low-lying coastal zones and river deltas (1), areas that are also of paramount importance for regional and global food security (2–4). The majority of the world's most productive and densely populated coastal areas, such as the deltas of the Mekong (5–7), Irrawaddy (8), Ganges-Brahmaputra (9), Nile (10), and Mississippi (11), are experiencing significant subsidence and land loss as a result of reduced sediment supply from upstream basins, unsustainable management of water and sediment in the deltas, and global sea-level rise (12, 13). The subsidence of these major deltas relative to rising sea levels foreshadows fundamental failures of critical food systems and livelihoods (1, 2, 12–14).

Hard engineering approaches maintain some heavily subsidized deltas (4) but come at the cost of major capital investments and lock-ins into unsustainable conditions (3, 15). An alternative is to maintain or increase the natural resilience of river deltas, i.e., their ability to recover from shocks and adapt to change through natural processes (3). The resilience of river deltas depends on a balance between processes that accelerate subsidence of the delta surface, sea-level rise, and land accretion driven by sediment supply from upstream rivers (2, 5, 13, 16, 17). Anthropogenic change is altering most of these processes, and impacts will increase in the future (1, 2, 12, 17, 18). For example, global sea levels are rising (1), unsustainable groundwater extraction is

widespread (10, 19, 20), and basin development is reducing sediment supply to many deltas (5, 16, 17, 21, 22).

As basin- and delta-scale processes are connected, an integrated perspective would be key to identifying strategies for improving the resilience of delta land and livelihoods. Basin and delta scales are still mostly disconnected, however, in both scientific studies and management plans. While some delta-scale studies have attempted to translate reduced sediment supply into measures of sea-level rise relative to the subaerial delta surface (relative sea-level rise, rSLR) (5, 16, 21), they were limited to few scenarios or qualitative assessments to estimate future sediment supply from contributing river basins. Moreover, they neither explored multiple possible futures of basin development nor accounted for the uncertain and competing drivers of sediment generation and transport in large river basins. More granular studies of basin development have, in turn, produced quantitative estimates of changing sediment supply from (sub)basin to global scales but were not coupled to models of delta morphology, key to translating changing sediment supplies into endpoint measures of rSLR and delta resilience (17, 18, 23–26).

Importantly, previous studies did not evaluate uncertainty in future sediment supply arising from competing and highly uncertain drivers. Available evidence suggests that sediment trapping in

Significance

Globally, river deltas, which support some of the planet's most productive agro-economic systems and half a billion livelihoods, are at risk of being drowned by rising sea levels and accelerated subsidence. Whether delta land falls below sea level will depend on land and water management in the delta, sediment supply from the upstream basin, and global climate change. Those drivers cover multiple scales and domains and are rapidly changing, uncertain, and interconnected, which makes finding robust strategies to increase the resilience of river deltas challenging. Herein, we demonstrate an approach to identify planning levers that can increase the resilience of river deltas under a wide range of future conditions for the 40,000-km² Mekong Delta in Southeast Asia.

Author contributions: R.J.P.S., M.G., S.B., G.M.K., G.C.D., and A.C. designed research; R.J.P.S., M.G., and S.B. performed research; R.J.P.S. and M.G. contributed new reagents/analytic tools; R.J.P.S. and M.G. analyzed data; and R.J.P.S., M.G., S.B., G.M.K., G.C.D., and A.C. wrote the paper.

Reviewers: F.E.D., Utrecht University; and D.P.L., Cornell University.

The authors declare no competing interest.

This open access article is distributed under Creative Commons Attribution-NonCommercial-NoDerivatives License 4.0 (CC BY-NC-ND).

¹To whom correspondence may be addressed. Email: rschmitt@stanford.edu or gdaily@stanford.edu.

This article contains supporting information online at <https://www.pnas.org/lookup/suppl/doi:10.1073/pnas.2026127118/-DCSupplemental>.

Published September 2, 2021.

past and future dams will outweigh increased sediment yields from climate and land-use change for most basins (17, 18). While this is an important finding, it comes from studies focused on full development of global hydropower potentials (27). This is a limitation, because decreasing prices of alternative renewables will likely reduce the demand for hydropower, thereby enabling strategic hydropower planning with least cumulative impacts (24, 25, 28, 29). Sediment trapping could also be reduced by optimized design and management of individual dam projects (30, 31). However, the cumulative benefits of such approaches have not been demonstrated at the scale of large basins, with many planned dams and under changing environmental conditions.

A framework that integrates basin and delta processes and accounts for their interactions and uncertainty in their future magnitude and direction could be used to design robust strategies to minimize rSLR and increase delta resilience. Here, we present such an integrated framework and demonstrate its application to the Mekong Basin and Delta (Fig. 1A). The framework combines a basin and delta component and builds on concepts of exploratory modeling and decision scaling (32–34). We use this framework to identify key drivers of rSLR in the Mekong Delta. Mostly less than 2 m above sea level (6), the Mekong Delta is globally outstanding in terms of supported livelihoods and food production (35). The Mekong Delta is also outstanding in terms of imminent threats across scales, from unsustainable groundwater use and land management (19, 20, 36–39) in the delta to upstream hydropower development (22, 40) and global climate change (5, 41), thus presenting a challenging and relevant case study.

Our framework helps to address three main research gaps. First, we study the sensitivity of rSLR to delta-scale drivers (DSDs, e.g., sea level rise and accelerated subsidence) and basin-scale drivers (sediment supply). Second, we analyze different scenarios of hydropower development in the basin with regard to their impacts on sediment supply. Using a basin model (25) we subject each hydropower scenario to many realizations of sediment yields and sediment trapping in dams. Third, we perform a bottom-up analysis linking sediment supply to hydropower development as well as to other basin-scale drivers, e.g. climate and land-use change (42, 43). Instead of prescribing a few scenarios we map the response of sediment supply to a wide range of basin-scale drivers and identify which combinations of those drivers are compatible with certain levels of sediment supply (42, 43) and thus certain levels of future resilient delta land.

Results

First, we explore different scenarios of DSDs and sediment supply (*Methods*) for the Mekong Delta. We then model for each of those scenarios how much of the delta surface would remain subaerial (i.e., above sea level) and how much would fall below sea level by 2100. For that, we deploy a conceptual model of delta morphodynamics (*Methods*), which translates DSDs and sediment supply into an aggregate measure of rSLR. The results allow us to explore if rSLR is more sensitive to DSDs or to sediment supply. Using recent topographic data (6), we also map which parts of the delta would fall below sea level for different values of rSLR.

Our estimates of rSLR range from 0.23 m to 1.39 m by 2100. Because of the extremely low topography of the delta, such rSLR would result in 7.4 to 89% loss of the subaerial delta land (i.e., land above sea level) (Fig. 1B). Relative sea level (rSLR) is influenced by DSDs more than by sediment supply, such that even with pristine sediment supply for the basin (~160 Mt/y) subaerial land would change by -7.4 and -76.2% (Fig. 1B, *Top*). However, sediment supply modulates how much delta land remains above sea level within each DSD scenario. Varying sediment supply between 160 and 5 Mt/y results in -7.4 to -26.9% (best-case DSD), -37.7 to -63.5% (central-case DSD), and -76.2

to -89.2% (worst-case DSD) of land above sea level (Fig. 1B and C). Thus, rSLR is most sensitive to sediment supply for the central case of DSDs, for which changes in sediment supply from 160 Mt/y (natural load) down to 5 Mt/y [with sediment trapping by full dam buildout (22)] produce a 25.8% variation in land above the sea level (37.7 to 63.5%). The same variation in sediment supply with the best-case DSD scenario results in a 19.5% variation (-7.4 to 26.9%), and the worst-case DSD scenario results in a 13% variation (76.2 to 89.2%). For the central-range DSD scenario, sediment supply makes the difference between large swaths of land along the southeastern shorelines and in the northeastern center of the delta falling below or remaining above the sea level. Stretches of the eastern delta would fall below sea level even under best-case DSDs (Fig. 1D, green). Worst-case DSDs would increasingly drown higher-lying areas along the distributary channels (Fig. 1D, light purple to orange).

Thus, rSLR and land above sea level is mostly controlled by delta-scale management of accelerated subsidence. However, sediment supply also plays an important role. Sediment supply will be reduced by dams (35), but the magnitude of reduction depends on where and how dams are built and operated (24, 25, 30, 31). Similarly, sand mining in the lower Mekong will reduce sediment supply (51), but how much depends on locations and rates of mining [subject to market forces and enforcement of government regulations (35)]. Also, road construction (44) and changing land use and climate (42, 43, 45) might alter sediment yields and thus how much sediment is supplied to rivers. However, especially for climate drivers the direction of change is uncertain and might differ throughout the basin (41).

To model joint impacts of changing sediment yields and dam siting we considered 17 different scenarios of dam siting. Each of the 17 scenarios represents a different portfolio of dams, i.e., a different set of dam sites, and is associated with one of 11 levels of increasing hydropower generation, referred to as generation levels 1 to 11 (GL1 to GL11). GL6 is the status quo, i.e., GL1 to GL5 represent the past construction of dams up to the current generation of 140,000 GWh/y at GL6 (Fig. 2A and B, purple). Starting from the existing dams at GL6, we analyzed two diverging trajectories for the future. The first trajectory results from a business-as-usual future of hydropower development (Fig. 2A and B, red). As an alternative, we analyzed dam portfolios optimized for connectivity between the delta and the basin, referred to as the Mekong Delta connectivity (MDC) sequence (25) (blue in Fig. 2A and B). We then subjected each of the 17 portfolios (one historic portfolio for GL1 to GL5 and two each for GL6 to GL11) to 130,000 Monte Carlo analysis (MCA) runs of the CASCADE network sediment model (25). In each run, we varied parameters for sediment yield from seven geomorphic provinces (22, 25) and for sediment trapping in the dams of five riparian countries (25) (*Methods*).

Our analysis advances studies of sediment trapping in Mekong dams (22, 25, 40), constraining the possible range of sediment supply for any dam portfolio (Fig. 2A). We estimate that sediment delivery to the delta with current dams can be around 58 ± 17 Mt/y (mean ± 1 SD over the 130,000 MCA runs) (Fig. 2A, GL6), with the variability originating from uncertain sediment supply and uncertain sediment trapping in existing dams. This reduction in sediment supply to the delta would result in an estimated -23 to -87% change in subaerial delta land by 2100 (Fig. 2A, GL6, right y axis).

Current plans for expanding hydropower focus on large dams in the lower Mekong tributaries and the mainstem of the Mekong in Laos and Cambodia (Fig. 2B, e.g., GL8, red markers). This would increase generation to around 194,000 GWh/y (GL8) but decrease sediment supply to 31 ± 13 Mt/y, with the tail of the distribution reaching 5 Mt/y. For full hydropower development (GL11) the mean sediment delivery to the delta is reduced to 9 ± 1.5 Mt/y. Such a reduction in sediment supply to

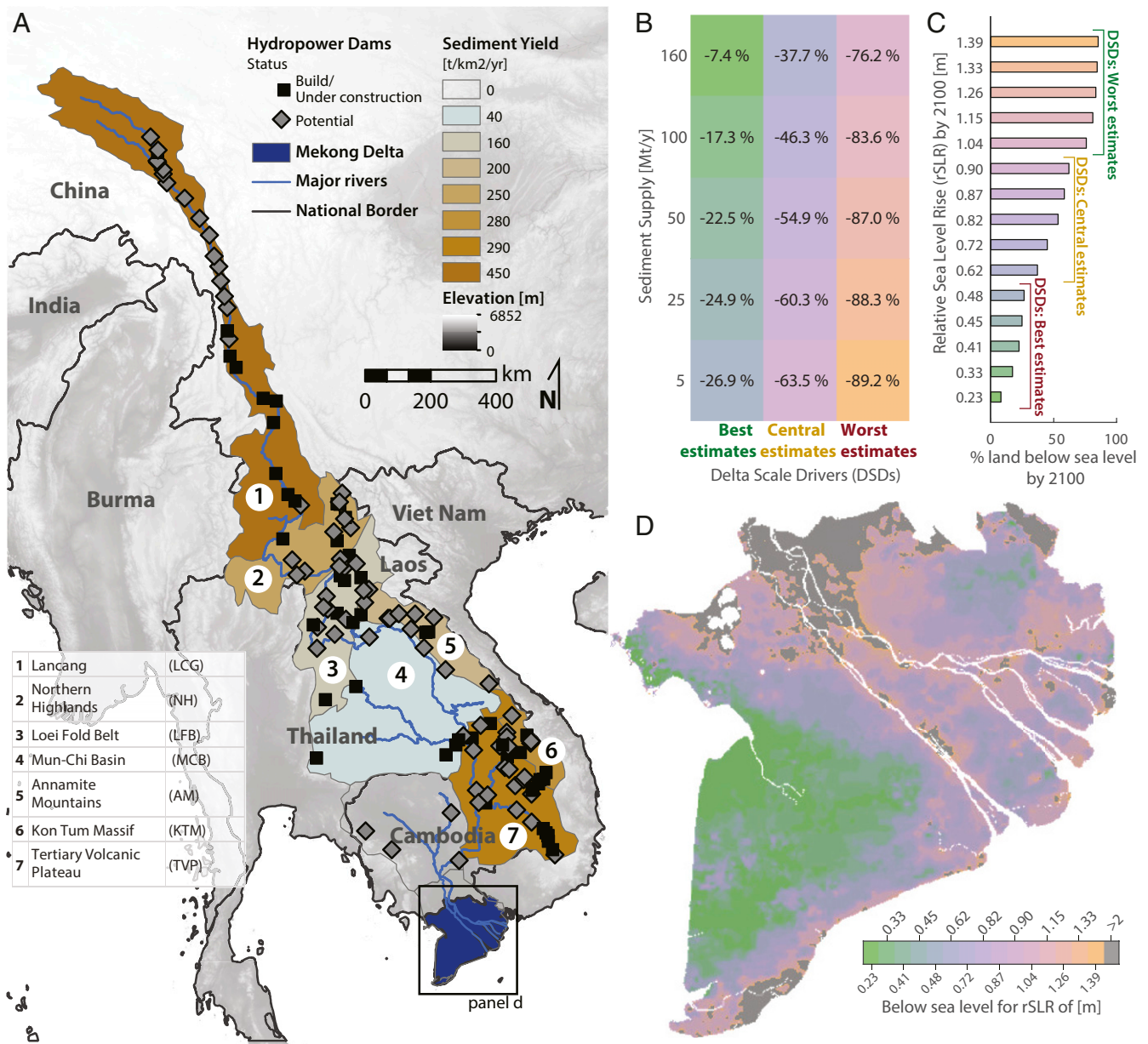


Fig. 1. Up to 90% of the Mekong Delta might fall below sea level by 2100. (A) The 800,000-km² Mekong basin can be divided into distinct geomorphic provinces (22) (numbers 1 to 7), each with a different contribution to the sediment budget of the basin. (B) Different levels of sediment supply from the basin (rows) together with different scenarios for DSDs (columns) result in different levels of rSLR (colors) and thus different fractions of the current delta surface remaining subaerial, i.e., above sea level (percentages). (C) The change in subaerial delta surface for each level of rSLR in B based on most recent topographic data (6). (D) These topographic data are used to locate areas below sea level. Refer to *SI Appendix, Fig. S2* for trajectories of subaerial delta surface from 2020 to 2100 and for continuous levels (0 to 160 Mt/yr) of sediment supply. Note that colors in B, C, and D are corresponding.

the delta would result in a 27 to 90% change in subaerial delta land. With more dams in the lower Mekong Basin sediment supply to the delta becomes less sensitive to changing sediment yields from hillslope processes and sediment trapping in dams (Fig. 2, see more and more narrow “violins” for GL8 to GL12). Thus, for the planned dam sequence even future increases in sediment yields and decreases in sediment trapping would not result in more sediment supply to the delta. This is because cumulative sediment trapping in large dams on the lower Mekong mainstem would outweigh additional sediment from changing catchment processes and better sediment passage through upstream dams.

The optimized dam portfolio for GL8 would consist mostly of dams upstream of existing dams, both in China and on lower

Mekong tributaries (Fig. 2B, GL8, blue markers). With that dam portfolio, sediment supply could be maintained at or slightly below the current rate. Beyond GL8, even optimized dam portfolios will lead to decreasing sediment supply. However, up to GL10, sediment supply is significantly higher for the MDC than for the currently planned sequence (compare violin plot for GL8, GL9, and GL10 for the MDC vs. planned sequence). Reaching GL8 following the MDC sequence would reduce the surface of the subaerial delta by –23 to –87%, compared to around –27 to –90% for the planned sequence (both for the central estimates of sediment supply).

The proliferation of dams in the basin not only reduces total sediment supply but also changes the sensitivity of sediment supply to basin-scale processes. In the past, when there were few

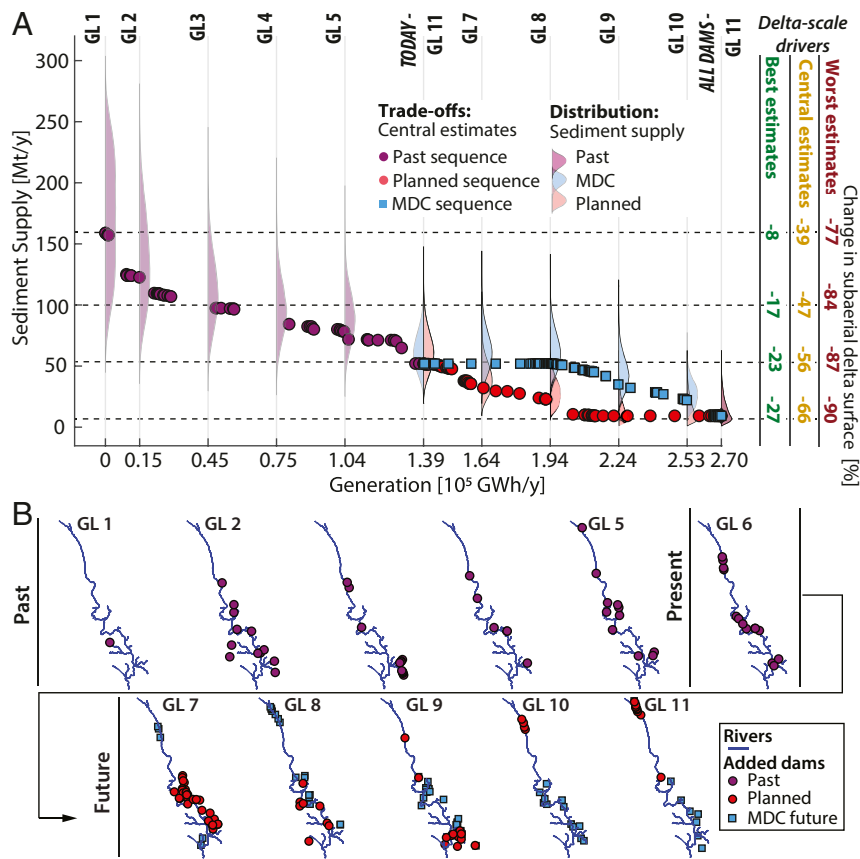


Fig. 2. Business-as-usual hydropower development will lead to significantly less sediment supply than strategic dam development. (A) Each point indicates the central estimate for sediment supply and hydropower for a specific dam portfolio. We selected 17 dam portfolios resulting in 11 distinct generation levels (GL1 to GL11) for a detailed analysis. For each of those portfolios, we estimated uncertainty in sediment supply using 130,000 Monte Carlo runs of a network sediment model. Violin plots for each portfolio demonstrate the statistical distribution of results. The right y axis links different levels of sediment supply to a reduction in the subaerial delta surface (i.e., land above sea level) by 2100. This reduction is shown for three different scenarios of DSDs (compare Fig. 1B). (B) Spatial layouts for past (purple) and future generation levels shown in A. Note that for the future there are two different scenarios for reaching each generation level: planned (red circles) and an optimized alternative (blue squares). See also *SI Appendix, Fig. S3*.

dams in the basin (GL1, Fig. 2B), sediment supply was most sensitive to sediment yields in the Lancang (Fig. 3A, GL1), the upper part of the basin in China (Fig. 1A). As large dams were built on the lower Lancang (GL2 to GL5, Fig. 2B), sediment supply to the delta became less sensitive to sediment yields in the Lancang. Instead, sensitivity to the sediment trapping in dams in China, i.e., the Lancang, increased (Fig. 4A, sediment trapping China for GL2 to GL4). Today, sediment supply is no longer sensitive to sediment trapping rates in the Chinese dams either. This is because dams in the Lancang are many and very large (Fig. 3A, GL6). Thus, cumulatively dams in the Lancang will trap most incoming sediment even if the trapping rates in individual dams in the Lancang were lower than expected. As the Lancang became more and more disconnected (Fig. 3A, GL4 to GL6), sediment supply became increasingly sensitive to sediment yields in the lower basin, notably the Tertiary Volcanic Plateau (TVP) in Laos and Vietnam and the Northern Highland of Laos (Fig. 1A).

If higher generation levels are achieved following the planned trajectory of hydropower development (Fig. 2B, red circles), most of the basin will be decoupled from the delta in the near future. If the planned sequence of dams would be developed up to GL8 (Fig. 2B, red circles) sediment supply would only be sensitive to yields in the TVP and to sediment trapping by dams in Laos and Cambodia (Fig. 3B, GL8). Sediment supply would remain sensitive to similar drivers for MDC sequence, which in

contrast mostly includes dams upstream of existing dams, for GL6 up to GL8.

We then map the response of sediment supply to continuous changes in the most sensitive drivers over the entire analyzed parameter range (Fig. 3D–G). We use these response maps in a bottom-up manner to estimate which combinations of basin-scale drivers are compatible with certain levels of sediment supply. Bottom-up studies on engineered systems often rely on well-defined thresholds for system success or failure (34) and response maps can identify conditions for either system success or failure. For a complex human–natural system, such as a river delta, there are no clear failure/success thresholds. Instead, delta resilience will continuously scale with sediment supply (Fig. 1B). Therefore, we herein use the central estimate of current sediment supply (58 Mt/y) as an illustrative threshold. We then study under which conditions this threshold would be met or exceeded. In the future, different thresholds can be derived from participatory processes or transboundary dialogues (32) and analyzed using this bottom-up approach.

We illustrate the bottom-up approach for GL8 following the MDC sequence. If sediment yields in the Lancang and TVP would decrease by 25% (Points A in Fig. 3D and F), mean sediment supply to the delta would decrease to an average of 50 Mt/y (Fig. 3D). The probability of attaining the 58 Mt/y threshold would be only around 25% (Fig. 3F). If sediment yields in the Lancang and TVP would increase by 25% (Points C in Fig. 3D

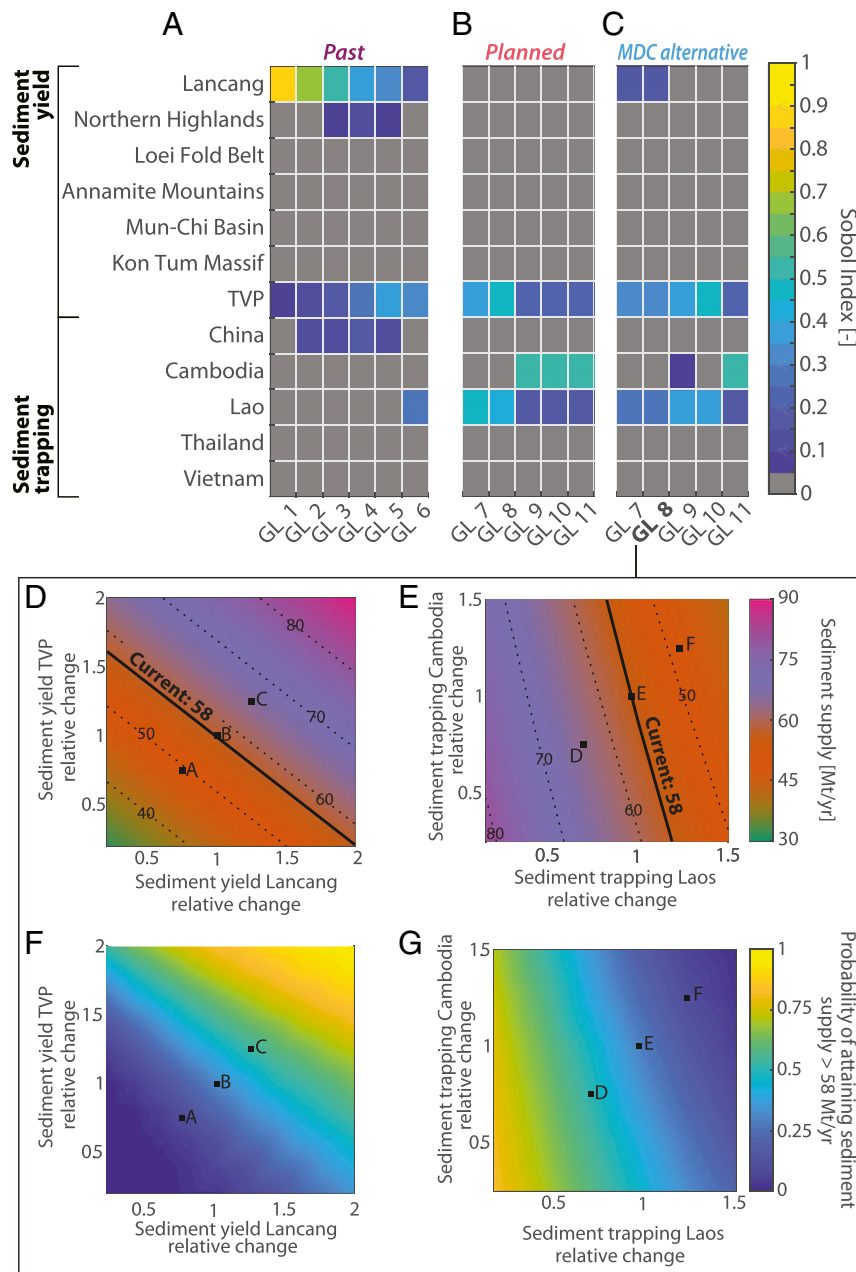


Fig. 3. Infrastructure decisions alter the impact of basin-scale drivers on sediment supply to the Mekong Delta. Sensitivity of sediment supply to the Mekong Delta and sediment trapping parameters for the past (A), the planned future (B), and the optimized MDC scenario (C). Sensitivity is measured as Sobol index, ranging from 0 (no sensitivity) to 1 (high sensitivity) computed over 130,000 MCA realizations for each dam portfolio (Fig. 2B). (D–G) The response of sediment supply to continuous changes in the most sensitive drivers for GL8 for the MDC sequence in terms of resulting mean sediment supply (D, E) and in terms of attaining at least the current level of supply (58 Mt/y). Points A and C mark a 25% decrease or increase in sediment yields compared to central estimates (Point B). Points D and F mark a 25% decrease or increase in sediment trapping compared to central estimates (Point E).

and F) mean sediment supply to the delta would increase to an average of 66 Mt/y (Fig. 3D). The probability of attaining the 58 Mt/y threshold would be 60%. Similar reasoning can be applied to sediment trapping in Laos and Cambodia. If sediment trapping in dams in both countries is 25% less (Point D in Fig. 3E and G) the central estimate of sediment supply would increase to around 64 Mt/yr (Point D in Fig. 3E) and the probability of attaining 58 Mt/y would be around 55%.

We can further analyze if the MDC sequence robustly results in a higher probability to attain the 58 Mt/y threshold compared with the planned sequence even under future uncertainty. With the planned sequence of dam construction, there is a very low

probability of attaining the 58 Mt/y threshold for most combinations of basin-scale drivers (Fig. 4A and B). The only possible case would be if sediment trapping in dams in Laos were less than half the central estimates and 58 Mt/y could be attained with around 50% probability (point A in Fig. 4B). By contrast, the MDC sequence would attain the 58 Mt/y threshold with the same probability for central estimates of sediment trapping (marker CE in Fig. 4C and D).

Fig. 4E and F show the difference in probabilities between the MDC and the planned sequence. This comparison highlights conditions of sediment yield and sediment trapping under which the MDC sequence would perform better than the planned

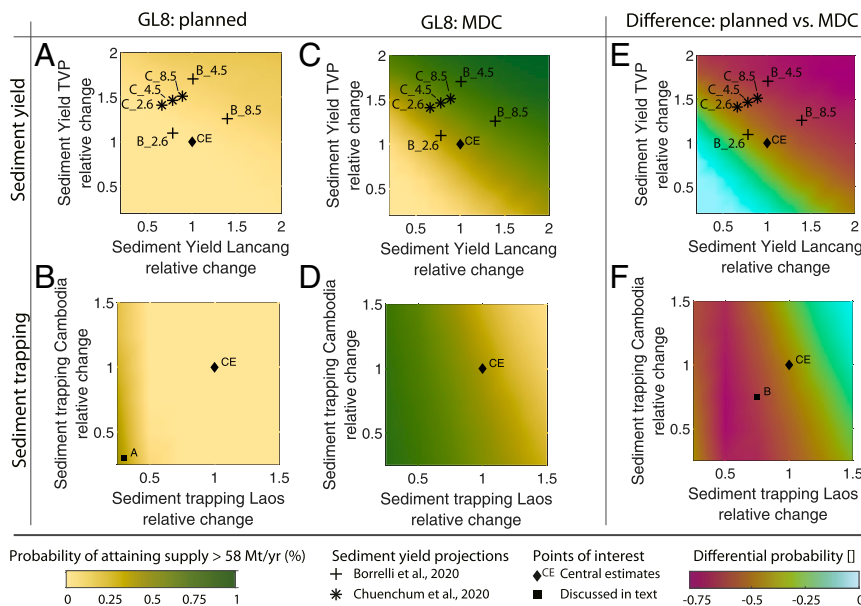


Fig. 4. Strategic planning is essential to leverage lower sediment trapping in dams and higher sediment yields for more sediment supply to the delta. (A and B) Probability of attaining current levels of sediment supply (58 Mt/y) with the planned dam sequence. (C and D) Same as A and B, but for the strategic MDC hydropower sequence. (E) Difference between A and C. (F) Difference between B and D. Cross and asterisk markers indicate projections of sediment yield from Borelli et al. (42) (+ markers) for the year 2070 and by Chuenchum et al. (43) (* markers) for the year 2030 using different RCPs and land-use scenarios. Numbers indicate the RCPs, prefixes “C_” and “B_” indicate projections from either Borrelli et al. (42) or Chuenchum et al. (43). Square markers A and B are discussed in the text.

sequence. Notably, the likelihood of the MDC sequence outperforming the planned sequence increases with more optimistic estimates of sediment yield and sediment trapping (yellow and purple in Fig. 4E and F). Importantly, we find no conditions under which the planned sequence outperforms the MDC sequence.

To constrain potential future changes in sediment yield, we analyzed projections of sediment yields by 2030 (43) and by 2070 (42) (SI Appendix, Supplemental Methods). Each assessment included different climate and land-use projections. Cross and star markers in Fig. 4A, C, and E indicate the projected relative change in sediment yields from the Lancang and the TVP. While there is considerable variability in projected sediment yields both datasets indicate a decrease in sediment yield in the Lancang and an increase for the TVP for moderate emission scenarios, e.g., RCP2.6 (Representative Concentration Pathway 2.6). Projections for RCP4.5 by Borelli et al. (42) (Fig. 4A, B_4.5) indicate a major increase in sediment yield from the TVP (+70%), while yields in the Lancang remain mostly stable (+8%). Projections from the same study for RCP8.5 (Fig. 4A, B_8.5) indicate instead a major increase in sediment yields from the Lancang (+40%) and a smaller increase in sediment yields in the TVP (+25%). Chuenchum et al.’s projections for RCP4.5 and RCP8.5 (Fig. 4, C_4.5 and C_8.5) indicate lower sediment yields from the Lancang (−22 and −11%) and increases in sediment yield from the TVP (+46 and +51%) (43).

Under B_4.5 and B_8.5, optimized dam portfolios would attain a sediment supply of 58 Mt/y with around 80% (B_4.5) and 65% probability (B_8.5) (Fig. 4B). Compared to our baseline (Fig. 4E, point CE) most projections (except B_2.6) would increase the probability of attaining the 58 Mt/y threshold. Notably, the MDC sequence has an even greater benefit for B_4.5 and B_8.5 than for the baseline conditions. Thus, changing sediment yields increase the advantage of the MDC sequence over the planned sequence in terms of attaining the 58 Mt/y threshold (B_4.5 and B_8.5 in Fig. 4E). Only if much less sediment is supplied to rivers does this advantage decrease (light blue in

Fig. 4E). Those conditions could occur if extreme weather events decrease in magnitude and frequency (41).

There are no projections of future sediment trapping in dams. On the one hand, stricter environmental safeguards might lead to designing and operating future dams for less sediment trapping compared our central estimates (31). On the other hand, many dams in the Mekong were built without large bottom outlets or other features needed for sediment management, which hinders future implementation of sediment management in existing dams (30). If improved sediment management in dams is possible in the future, the cumulative benefits of those dam-scale measures need to be leveraged by strategic hydropower planning. The relative advantage of the MDC sequence (Fig. 4D) over the planned sequence (Fig. 4B) increases from 40% (Fig. 4F, CE) to nearly 60% if sediment trapping in dams is reduced by 25% compared to the central estimate (Fig. 4F, B).

Discussion

Globally, coastal populations are growing (1, 2), and climate change (1) and major infrastructure plans (14, 17, 27) threaten the resilience of many large river deltas. Our results from the Mekong Delta, which supports more than 17 million livelihoods and food systems of global importance (35), point to the need for sustainable land, water, and sediment management on delta and basin scales. While river basin and delta processes are commonly disconnected in research and management, our findings highlight the importance of integrating assessments across scales to estimate future rSLR and to identify effective management levers for achieving delta resilience in a robust manner.

Our results from integrating basin- and delta-scale models emphasize that rSLR in the Mekong Delta will be driven by accelerated subsidence from unsustainable groundwater abstractions (5, 19, 20, 36, 38). The area of the delta remaining above raising sea levels will change by −23 to −87% by 2100, even if sediment supply stays at or close to current levels (around 58 Mt/y). Delta planning must consider this imminent threat to agriculture and other livelihoods and the potential for permanent land loss.

Despite the dominance of DSDs, maximizing sediment supply is crucial to maintain at least some delta land above sea level (3, 4, 12), especially if DSDs are managed more sustainably in the future. Integrated planning is thus needed to evaluate future decisions in the basin regarding their impacts on delta resilience and comparing monetary benefits from development activities, e.g., hydropower or sand mining, to costs of adaptation, relocation, and coastal engineering in the delta.

Strategic infrastructure planning is paramount for maintaining sediment supply to the Mekong Delta (22, 24, 25, 40) and thus for maximizing its resilience. Specifically, further business-as-usual dam development is not compatible with maintaining sediment supply even at the current levels, which are strongly reduced compared to the basin's pristine state. Only strategic dam planning across all riparian countries could produce a modest increase in hydropower generation while maintaining sediment supply close to current levels. Our analyses highlight that strategic infrastructure planning on a portfolio level is a robust strategy to minimize cumulative environmental impacts of dams even under major uncertainty. This finding has implications beyond the Mekong because most of the global hydropower potential is in large and poorly studied basins, where origins of sediment and other natural values are poorly constrained and subject to change, and where the design and operation of future dams is highly uncertain (27).

For the Mekong, our results indicate that better design and management of individual dams is unlikely to translate into better sediment supply if dams are not developed in a strategic manner. Of course, environmental safeguards on the scale of individual dams can alleviate local negative externalities and might seem more practical from a political perspective than a basin-scale planning process. However, our results show that only strategic planning on a portfolio level ensures that local safeguards, such as better sediment management, result in basin-scale improvements in environmental objectives.

Our analyses relied on a multistage exploratory process to constrain most significant drivers of rSLR and to focus the analysis on drivers with the greatest relative uncertainty. However, future research could include the entire connected system model, i.e., including both basin and delta processes, into the bottom-up analysis. Ideally, future analyses would also improve process representation in the delta to capture the spatial heterogeneity in groundwater extraction and natural compaction (19, 20, 38, 46), as well as feedbacks between delta management and sediment accretion (39). Results could then be used by regional stakeholders to negotiate trade-offs and to develop adaptation plans (47) that consider realistic levels of future rSLR and acknowledge the intrinsic links between processes on delta, basin, and global scales.

Making deltas more resilient will require navigating conflicting objectives on multiple scales, within overarching uncertainties and shocks from global climate change and collapse of nature. Integrating parsimonious models that jointly represent deltas and their contributing basins can provide critical information to make delta management robust to future uncertainty and help in establishing delta resilience as a crucial objective in river basin management.

Methods

We base our analyses on three main components. First, we developed a conceptual morphodynamic model of the Mekong Delta, which, in contrast to previous iterations (5), considers dynamic feedbacks between land loss and aggradation. This model allows us to transfer basin and DSDs into a common metric of rSLR. We then use the latest topography of the Mekong Delta (6) to identify which areas would fall below sea level for different rates of rSLR (e.g., Fig. 1). Throughout the paper, this model is used to translate sediment supply rates into estimates delta surface below sea level by the end of the century.

Second, we use a network-scale sediment routing model (25, 48) to analyze impacts of changing sediment yields and dam sediment trapping on sediment supply. We use the model to simulate different scenarios of dam

development. For each scenario, we perform an MCA, consisting of 130,000 runs of the basin model. In each run, the model implements a new combination of sediment yields from seven geomorphic provinces and dam sediment trapping in five riparian countries.

Finally, we implement a variance-based sensitivity analysis (49, 50) to determine sensitivity of sediment supply to a total of 12 different parameters for each of the 17 dam portfolios.

Delta Plane Model. The delta plane model (5) is used to estimate future subaerial land in the Mekong Delta for different combinations of basin and DSDs. The delta plane model is based on a sediment mass balance for the delta, which then allows us to put changes in sediment supply (in megatons per year) and accelerated subsidence (in millimeters per year) into a common metric of rSLR (in millimeters per year). The model is run with annual timesteps to 2100.

In each year, subsidence of the delta plane because of local drivers is determined as

$$SUBS(t) = CMP(t) + PMP(t),$$

where *SUBS* is total subsidence, *CMP* is natural compaction, and *PMP* is subsidence from groundwater pumping (all in millimeters per year) at time *t* [years]. Subsidence is counteracted by sediment supply from the basin, which accretes delta land as it spreads out over the delta surface. The effect of this land building is expressed as

$$ACC(t) = \frac{SED^*(t)}{\rho_s} * \frac{1}{A_{Delta}(t)},$$

where *SED** is the sediment supply (tons per year), ρ_s is the density of deposited material (tons per cubic meter), *A_{Delta}* is the subaerial extend of the delta (square meters), and *ACC* is the resulting accretion. Note that *SED** considers for the effect of sand mining

$$SED^* = \max(0, SED(t) - MNG(t)).$$

Thus, if rates of mining (*MNG*) exceed sediment supply, there will be no more supply to the delta, but the rate of supply cannot become negative. In reality erosion could replace parts of the mined sediment, i.e., increasing sediment supply at the cost of incision and lateral erosion of river channels and associated negative externalities (51, 52).

For both mining and pumping, we assume that rates will decrease over time, both because of stricter environmental regulations and possible land loss and decreasing agricultural area, so that

$$PMP(t) = PMP(t = 0) * m^t$$

and

$$MNG(t) = MNG(t = 0) * m^t,$$

where *m* < 1 denotes a rate factor [–].

Finally, rates of rSLR in each time step can be determined as

$$rSLR(t) = SLR(t) + SUBS(t) - ACC(t)$$

and the cumulative rSLR is then

$$rSLR_{tot}(t) = \sum_{k \in \{1, \dots, t-1\}} rSLR_{tot}(k),$$

which can be compared to recent topographic data (Fig. 1E) (6) and a hypsometric curve of the delta (SI Appendix, Fig. S1) to identify which parts of the delta fall below sea level, and where those parts are located.

Dynamic versus Static Delta Plane Model. As indicated above, accretion rates will depend upon the subaerial delta surface on which sediment can accrete. In a static formulation, we assume that $A_{Delta}(t) = const = 40,000 * 10^6 m^2$. In a dynamic formulation, we assume that the area of the subaerial delta is variable, decreasing with increasing cumulative rSLR. As the supplied sediment will then spread over less area, the marginal accretion (i.e., in millimeters per ton) resulting from sediment supply will increase as the delta shrinks (5, 21, 53).

To estimate the subaerial delta land, we use the gridded digital elevation model of the delta provided by Minderhoud et al. (6) (SI Appendix, Fig. S1 shows the hypsometric curve of the delta plane). We calculate delta land remaining above sea level as

$$A_{\text{Delta}}(t) = \sum_{h(j) > rSLR_{\text{tot}}(t)} i^* c_j,$$

where i denotes a cell in the digital elevation model of the delta and c_j is the cell size of that cell (square meters). Thus, we form the sum of all cells that above the sea level rise for time t .

We derive a value of $rSLR$ for both dynamic and static model formulations $rSLR_{\text{tot,dyn}}(t)$ and $rSLR_{\text{tot,stat}}(t)$ by the year 2100 (SI Appendix, Fig. S2). Results are reported as the mean of the two models in the year 2100. We take this approach because neither the static nor the dynamic models is more realistic per se. Rather, we propose that the two models present an extreme envelope for accretion. Thus, $rSLR$ is calculated as

$$rSLR_{\text{tot}}(2100) = \frac{rSLR_{\text{tot,dyn}}(2100) + rSLR_{\text{tot,stat}}(2100)}{2}.$$

We separately report the outcomes of each model in SI Appendix, Fig. S2.

Similar to ref. 5, we propose three different scenarios for global and local drivers of subsidence. These drivers are natural subsidence, pumping, sand mining, and sea level rise. Each of the scenarios combines either a minimum, maximum, or central estimate value for each driver, all derived from reviewing pertinent published data (5). The ambition of this analysis is not to model the detailed morphologic development of the future delta but rather to provide a backdrop for how different rates of sediment supply, which couple the basin and the delta models, together with DSDs, will create very different futures for the delta.

The delta plane model comes with some relevant simplifications. First, we assume that sediment is spread across the entire delta surface. In a natural delta, areas closer to rivers and depressions would receive more deposition. In a heavily modified delta, sediment deposition is further altered by infrastructure for irrigation and flood protection (39). Second, we assume that DSDs are constant in space. Instead, new research indicates spatial variability, e.g., in natural compaction and pumping-related subsidence (19, 20, 36, 37, 46). Third, the model considers neither the role and dynamics of different grain sizes, e.g., sand from natural bed-load transport versus finer sediment from hillslope processes, nor off-shore sediment transport (54). These points call for efforts to build spatially explicit models for delta management, which could draw on recent spatial datasets of subsidence (6, 36, 38, 46). Finally, estimates for some drivers might seem dire but are still optimistic with regard to local management, as we assume decreasing trends of unsustainable groundwater use and sand mining. While this assumption is in line with mitigation scenarios proposed in other papers (36), irrigation abstractions are still increasing in parts of the delta (55), highlighting the need for better water management in the delta.

Sediment Routing and Trapping Model. The functioning of the model used for this analysis is described elsewhere (25). In a nutshell, the model uses a graph-based routing scheme to represent transport of sediment from each node in the river network to the basin outlet. The sediment supply (in tons per year) at each source node ζ [denoted $y(\zeta)$] is determined by the local sediment yield (in tons per square kilometer per year) and the area supplying sediment to the node (in square kilometers). The local sediment yield is determined by its location within one of seven geomorphic provinces.

Sediment trapping rates for each dam are determined by applying the Brune curve (56). According to the nonlinear Brune model, sediment trap efficiency in a dam, $TE(d)$, is a function of hydraulic residence time in the associated reservoir, which can be derived for current and future dams from available regional datasets (25).

Thus, the sediment routing model has a total of 131 parameters. First, there are 124 estimates of trap efficiency in dams. Then, there are estimates of sediment yield at each node in the river network, but as sediment yield is

assumed constant in each geomorphic province, yield parameters collapse to seven values, one for each geomorphic province.

Global Sensitivity Analysis. To test model sensitivity to these parameters, we applied a Sobol sensitivity analysis, a variance decomposition approach that attributes variance in the simulated model output to individual input parameters and their interactions (49, 50). Sampling the full space of all 131 input parameters would have resulted in an infeasibly large number of model simulations. Thus, we grouped the dams of each country together and defined a country-specific multiplier for the trap efficiency of dams in each country c . Using this multiplier, $\epsilon_{TE}(c)$, also reflects that environmental regulations for dam design and operation and requirements for sediment passage would potentially be enacted on a national level. Thus, for the sensitivity analysis, sediment trapping in a dam is determined by

$$TE'(d) = \epsilon_{TE}(c) * TE(d),$$

i.e., the central estimate of sediment trapping derived from dam-specific parameters and a country-specific multiplier. It should be noted that more detailed future studies for, e.g., smaller dam portfolios on specific tributaries, could adopt a similar approach on a single-dam level.

Similarly, the sediment yield at each node is modified by a multiplier that is specific to the geomorphic province, g . Using this multiplier, $\epsilon_y(g)$, allows us to modify the central estimates of sediment yield so that

$$y'(\zeta) = \epsilon_y(g) * y(\zeta),$$

where g is the geomorphic province in which source node ζ is located.

Scenarios of sediment supply and sediment trapping are then generated through a two-step scheme to sample the 12-dimensional parameter space (five countries and seven geomorphic provinces). For that, we used Sobol quasi-random sampling coupled with Saltelli's cross-sampling method (57) aimed at uniformly covering the multidimensional input space of ϵ parameters (49). We set the range of ϵ_{TE} to 0.25 to 1.5 and the range of ϵ_y to 0.2 to 2. Note that higher values of ϵ_{TE} represent more sediment trapping and thus less supply to the delta, while higher values of ϵ_y will lead to more sediment supply to the delta. Note that we capped ϵ_{TE} at a lower value (1.5) than ϵ_y (2.0). This is mostly because we propose that most uncertainty in sediment trapping is due to the unknown design and operation of run-of-river dams on the lower Mekong. For those dams, which might be partially drawn down during the flood season, sediment trapping is likely to be lower than the estimates derived from the Brune curve.

In total, we generated 130,000 inputs sets from the Sobol sequence and simulated the resulting sediment supply to the delta for 17 portfolios (five portfolios representing past dam development, six for the planned future, and six for MDC futures), for a total of 2,210,000 runs.

We then use Sobol indices to determine the sensitivity of the response variable (sediment supply) to each of the 12 model parameters. Both the input sampling and the Sobol sensitivity analysis were implemented using the MOEA Framework (50).

Data Availability. Data on dam location and design (25), delta topography (6), and global projections of sediment yields (42) are available from repositories associated with the respective publications. Color maps for Fig. 4 are available from Cramer (58). New geospatial data (geomorphic provinces) and code and data required to reproduce the robust analysis for future dam portfolios are available from Zenodo at <https://doi.org/10.5281/zenodo.5138143> (59). All other study data are included in the article and/or SI Appendix.

1. IPCC, "Summary for policymakers" in *IPCC Special Report on the Ocean and Cryosphere in a Changing Climate*, H.-O. Pörtner et al., Eds. (International Panel on Climate Change, 2019), pp. 3–35.
2. Z. D. Tessler et al., ENVIRONMENTAL SCIENCE. Profiling risk and sustainability in coastal deltas of the world. *Science* **349**, 638–643 (2015).
3. A. J. F. Houtink, et al., Resilience of river deltas in the Anthropocene. *J Geophys. Res. Earth Surface* **125**, e2019JF005201 (2020).
4. D. P. Loucks, Developed river deltas: Are they sustainable? *Environ. Res. Lett.* **14**, 113004 (2019).
5. R. J. P. Schmitt, Z. Rubin, G. M. Kondolf, Losing ground—Scenarios of land loss as consequence of shifting sediment budgets in the Mekong Delta. *Geomorphology* **294**, 58–69 (2017).
6. P. S. J. Minderhoud, L. Coumou, G. Erkens, H. Middelkoop, E. Stouthamer, Mekong delta much lower than previously assumed in sea-level rise impact assessments. *Nat. Commun.* **10**, 3847 (2019).

7. E. J. Anthony et al., Linking rapid erosion of the Mekong River delta to human activities. *Sci. Rep.* **5**, 14745 (2015).
8. D. Chen et al., Recent evolution of the Irrawaddy (Ayeyarwady) Delta and the impacts of anthropogenic activities: A review and remote sensing survey. *Geomorphology* **365**, 107231 (2020).
9. M. Becker et al., Water level changes, subsidence, and sea level rise in the Ganges-Brahmaputra-Meghna delta. *Proc. Natl. Acad. Sci. U.S.A.* **117**, 1867–1876 (2020).
10. E. Gebremichael et al., Assessing land deformation and sea encroachment in the Nile Delta: A radar interferometric and inundation modeling approach. *J. Geophys. Res. Solid Earth* **123**, 3208–3224 (2018).
11. J. A. Nittrouer, E. Viparelli, Sand as a stable and sustainable resource for nourishing the Mississippi River delta. *Nat. Geosci.* **7**, 350–354 (2014).
12. J. P. M. Syvitski et al., Sinking deltas due to human activities. *Nat. Geosci.* **2**, 681–686 (2009).

13. L. Giosan, J. Syvitski, S. Constantinescu, J. Day, Climate change: Protect the world's deltas. *Nature* **516**, 31–33 (2014).
14. C. Hill *et al.*, "Hotspots of present and future risk within deltas: Hazards, exposure and vulnerability" in *Deltas in the Anthropocene*, C. W. Hutton, R. J. Nicholls, S. Hanson, Eds. (Palgrave Macmillan, Cham, 2020), pp. 127–151.
15. A. C. Welch, R. J. Nicholls, A. N. Lázár, Evolving deltas: Coevolution with engineered interventions. *Elementa* **5**, 49 (2017).
16. Z. D. Tessler, C. J. Vörösmarty, I. Overeem, J. P. M. Syvitski, A model of water and sediment balance as determinants of relative sea level rise in contemporary and future deltas. *Geomorphology* **305**, 209–220 (2018).
17. F. E. Dunn, *et al.*, Projections of declining fluvial sediment delivery to major deltas worldwide in response to climate change and anthropogenic stress. *Environ. Res. Lett.* **14**, 084034 (2019).
18. J. P. M. Syvitski, C. J. Vörösmarty, A. J. Kettner, P. Green, Impact of humans on the flux of terrestrial sediment to the global coastal ocean. *Science* **308**, 376–380 (2005).
19. P. S. J. Minderhoud *et al.*, Impacts of 25 years of groundwater extraction on subsidence in the Mekong delta, Vietnam. *Environ. Res. Lett.* **12**, 064006 (2017).
20. L. E. Erban, S. M. Gorelick, H. A. Zebker, Groundwater extraction, land subsidence, and sea-level rise in the Mekong Delta, Vietnam. *Environ. Res. Lett.* **9**, 084010 (2014).
21. M. D. Blum, H. H. Roberts, Drowning of the Mississippi Delta due to insufficient sediment supply and global sea-level rise. *Nat. Geosci.* **2**, 488–491 (2009).
22. G. M. Kondolf, Z. K. Rubin, J. T. Minear, Dams on the Mekong: Cumulative sediment starvation. *Water Resour. Res.* **50**, 5158–5169 (2014).
23. F. E. Dunn *et al.*, Projections of historical and 21st century fluvial sediment delivery to the Ganges-Brahmaputra-Meghna, Mahanadi, and Volta deltas. *Sci. Total Environ.* **642**, 105–116 (2018).
24. R. J. P. Schmitt, S. Bizzi, A. Castelletti, G. M. Kondolf, Improved trade-offs of hydropower and sand connectivity by strategic dam planning in the Mekong. *Nat. Sustain.* **1**, 96–104 (2018).
25. R. J. P. Schmitt, S. Bizzi, A. Castelletti, J. J. Opperman, G. M. Kondolf, Planning dam portfolios for low sediment trapping shows limits for sustainable hydropower in the Mekong. *Sci. Adv.* **5**, eaaw2175, 10.1126/sciadv.aaw2175 (2019).
26. G. Grill *et al.*, Mapping the world's free-flowing rivers. *Nature* **569**, 215–221 (2019).
27. C. Zarfl, A. E. Lumsdon, J. Berlekamp, L. Tydecks, K. Tockner, A global boom in hydropower dam construction. *Aquat. Sci.* **77**, 161–170 (2014).
28. G. Ziv, E. Baran, S. Nam, I. Rodriguez-Iturbe, S. A. Levin, Trading-off fish biodiversity, food security, and hydropower in the Mekong River Basin. *Proc. Natl. Acad. Sci. U.S.A.* **109**, 5609–5614 (2012).
29. R. J. P. Schmitt, N. Kittner, G. M. Kondolf, D. M. Kammen, Joint strategic energy and river basin planning to reduce dam impacts on rivers in Myanmar. *Environ. Res. Lett.*, in press.
30. T. B. Wild, D. P. Loucks, Managing flow, sediment, and hydropower regimes in the Sre Pok, Se San, and Se Kong Rivers of the Mekong basin. *Water Resour. Res.* **50**, 5141–5157 (2014).
31. T. B. Wild, P. M. Reed, D. P. Loucks, M. Mallen-Cooper, E. D. Jensen, Balancing hydropower development and ecological impacts in the Mekong: Tradeoffs for Sambor Mega Dam. *J. Water Resour. Plan. Manage.* **145**, 05018019 (2019).
32. N. L. Poff *et al.*, Sustainable water management under future uncertainty with eco-engineering decision scaling. *Nat. Clim. Chang.* **6**, 25–34 (2016).
33. T. Hashimoto, D. P. Loucks, J. R. Stedinger, Robustness of water resources systems. *Water Resour. Res.* **18**, 21–26 (1982).
34. C. Brown, Y. Ghile, M. Laverty, K. Li, Decision scaling: Linking bottom-up vulnerability analysis with climate projections in the water sector. *Water Resour. Res.* **48**, W09537 (2012).
35. G. M. Kondolf *et al.*, Changing sediment budget of the Mekong: Cumulative threats and management strategies for a large river basin. *Sci. Total Environ.* **625**, 114–134 (2018).
36. P. S. J. Minderhoud, H. Middelkoop, G. Erkens, E. Stouthamer, Groundwater extraction may drown mega-delta: Projections of extraction-induced subsidence and elevation of the Mekong delta for the 21st century. *Environ. Res. Commun.* **2**, 011005 (2020).
37. K. de Wit *et al.*, Identifying causes of urban differential subsidence in the Vietnamese Mekong Delta by combining InSAR and field observations. *Remote Sens.* **13**, 189 (2021).
38. P. S. J. Minderhoud *et al.*, The relation between land use and subsidence in the Vietnamese Mekong delta. *Sci. Total Environ.* **634**, 715–726 (2018).
39. A. D. Chapman, S. E. Darby, Dams and the economic value of sediment in the Vietnamese Mekong Delta. *Ecosyst. Serv.* **32**, 110–111 (2018).
40. M. Kummu, X. X. Lu, J. J. Wang, O. Varis, Basin-wide sediment trapping efficiency of emerging reservoirs along the Mekong. *Geomorphology* **119**, 181–197 (2010).
41. S. E. Darby *et al.*, Fluvial sediment supply to a mega-delta reduced by shifting tropical-cyclone activity. *Nature* **539**, 276–279 (2016).
42. P. Borrelli *et al.*, Land use and climate change impacts on global soil erosion by water (2015–2070). *Proc. Natl. Acad. Sci. U.S.A.* **117**, 21994–22001 (2020).
43. P. Chuenchum, M. Xu, W. Tang, Predicted trends of soil erosion and sediment yield from future land use and climate change scenarios in the Lancang–Mekong River by using the modified RUSLE model. *Int. Soil and Water Cons. Res.* **8**, 213–227 (2020).
44. R. C. Sidle, A. D. Ziegler, The dilemma of mountain roads. *Nat. Geosci.* **5**, 437–438 (2012).
45. B. Shrestha, T. A. Cochrane, B. S. Caruso, M. E. Arias, Land use change uncertainty impacts on streamflow and sediment projections in areas undergoing rapid development: A case study in the Mekong Basin. *Land Degrad. Dev.* **29**, 835–848 (2018).
46. C. Zoccarato, P. S. J. Minderhoud, P. Teatini, The role of sedimentation and natural compaction in a prograding delta: Insights from the mega Mekong delta, Vietnam. *Sci. Rep.* **8**, 11437 (2018).
47. J. H. Kwakkel, M. Haasnoot, W. E. Walker, Developing dynamic adaptive policy pathways: A computer-assisted approach for developing adaptive strategies for a deeply uncertain world. *Clim. Change* **132**, 373–386 (2015).
48. R. J. P. Schmitt, N. Kittner, G. M. Kondolf, D. M. Kammen, Joint strategic energy and river basin planning to reduce dam impacts on rivers in Myanmar. *Environ. Res. Lett.* **16**, 054054 (2021).
49. I. M. Sobol, Global sensitivity indices for nonlinear mathematical models and their Monte Carlo estimates. *Math. Comput. Simul.* **55**, 271–280 (2001).
50. D. Hadka, P. Reed, Borg: An auto-adaptive many-objective evolutionary computing framework. *Evol. Comput.* **21**, 231–259 (2013).
51. C. R. Hackney *et al.*, River bank instability from unsustainable sand mining in the lower Mekong River. *Nat. Sustain.* **3**, 217–225 (2020).
52. M. G. Kondolf, Geomorphic and environmental effects of instream gravel mining. *Landsc. Urban Plan.* **28**, 225–243 (1994).
53. W. I. Van De Lageweg, A. B. A. Slangen, Predicting dynamic coastal delta change in response to sea-level rise. *J. Mar. Sci. Eng.* **5**, 24 (2017).
54. M. Besset, E. J. Anthony, G. Brunier, P. Dussouillez, Shoreline change of the Mekong River delta along the southern part of the South China Sea coast using satellite image analysis (1973–2014). *Géomorphologie: relief, processus, environnement* **22**, 137–146 (2016).
55. T. Hamer, C. Dieperink, V. P. D. Tri, H. S. Otter, P. Hoekstra, The rationality of groundwater governance in the Vietnamese Mekong Delta's coastal zone. *Int. J. Water Resour. Dev.* **36**, 127–148 (2020).
56. G. M. Brune, Trap efficiency of reservoirs. *Eos (Wash. D.C.)* **34**, 407–418 (1953).
57. A. Saltelli, *et al.*, *Global Sensitivity Analysis: The Primer* (John Wiley & Sons, 2008).
58. F. Cramer, Scientific colour maps. Zenodo. <https://zenodo.org/record/4491293#.YQ7-B7UBOIPY>. Accessed 17 May 2021.
59. R. J. P. Schmitt, Strategic basin and delta planning increases the resilience of the Mekong Delta under future uncertainty [Data set]. Zenodo. <https://doi.org/10.5281/zenodo.5138143>. Deposited 26 July 2021.